$2H_2O$ and (Δ)-β,γ-bidentate $Co((NH_3)_4H_2P_3O_{10}\cdot H_2O$. The two cobalt chelate rings are almost identical, differing chiefly in the amplitude of pucker: $Q = 0.623$ Å vs. $Q = 0.503$ Å, respectively. The amplitude of pucker in the present chromium complex is intermediate between the two cobalt complexes. However, the pseudorotation phase angle ϕ is 72° and 68° in the two cobalt rings (twist boat), which allows the phosphate oxygens projecting axially from the ring to hydrogen bond across the top and bottom of the chelate ring to the axial ammine ligands. The N···O distances in these hydrogen bonds range from 3.003 to 3.116 Å. Instead the chromium ring is 120° away on the pseudorotation cycle at $\phi = 306.7$ (3)°, which precludes the formation of interligand hydrogen bonds. The principal factor affecting the cobalt–ammine chelate ring conformation in the crystal structures is the interligand hydrogen bonding just mentioned. In solution the chromium complex may also assume a conformation stabilized by interligand hydrogen bonding with pseudorotation phase ϕ similar to the cobalt–ammine complexes. To do so, however, the chelate ring would have to increase its amplitude of pucker to bring the interligand separation into O···O hydrogen-bonding distance.

The six-membered chelate ring in these complexes is free to pseudorotate along the cycle of boat and twist-boat conformations. The energetically favored conformations along this path are determined by the hydrogen-bonding environment. When the axial position in the metal's coordination sphere can be occupied by nitrogen, as in the cobalt–ammine complexes, or when the metal is complexed with functional groups at an enzyme's substrate-binding site, then the possibility of stabilizing N···O hydrogen bonding across the top and bottom of the ring favors the twist-boat conformations at $\phi = 70°$ and $\phi = 250°$.[4] When the axial ligands are waters the enzyme could introduce strain in the phosphodiester bonds by increasing the amplitude of ring pucker, thus shortening the distance from the phosphate oxygens to the axial water ligands to allow the formation of hydrogen bonds.

With magnesium substrates (MgPP, MgADP, MgATP), where the coordination half-life is short, a functional group from the enzyme itself might replace an axially liganded water upon substrate binding. The enzyme functional group could then participate in interligand hydrogen bonding directly. This is not the case for the much more stable substitution-inert Co(III) and Cr(III) complexes, and enzymes for which these are acceptable substrates thus do not require such direct chelation to the metal. However, the enzyme may provide hydrogen-bond donors (or acceptors) which are not themselves liganded, and these may act to stabilize particular substrate conformations other than the twist-boat forms with attendant interligand hydrogen bonding. The extensive hydrogen-bonding network in the present structure may illustrate this. Evidence that the enzyme (kinases in the case of metal–ATP and pyrophosphatase in the case of metal–PP) does act as a hydrogen-bond donor in this fashion may be provided by the observation that the tetraaminecobalt and tetraaminechromium complexes bind very poorly to these enzymes on the whole,[10] while the tetraaquochromium complexes bind as tightly as the corresponding magnesium complexes.[3] The poorer binding may also be due to the liganded waters acting as acceptors for enzyme-donated hydrogen bonds, which the liganded ammonia cannot accept.

Acknowledgment. Research supported by NIH Grant GM-17378 to M.S. and NIH Biomedical Research Support Grant, University of Maryland, to D.D., who also acknowledges the Research Corp. and the donors of the Petroleum Research Fund, administered by the American Chemical Society, for partial support.

Supplementary Material Available: Listings of anisotropic thermal parameters and of structure factors (9 pages). Ordering information is given on any current masthead page.

(10) Janson, C. A.; Cleland, W. W. *J. Biol. Chem.* **1974**, *249*, 2562, 2567, 2572.

Proton Nuclear Magnetic Resonance Study of the Relaxation Behavior and Kinetic Lability of Exchangeable Protons in the Heme Pocket of Cyanometmyoglobin

John D. Cutnell,[1] Gerd N. La Mar,* and Stephen B. Kong

Contribution from the Department of Chemistry, University of California, Davis, California 95616. *Received November 7, 1980*

Abstract: The z-magnetization recovery times for several hyperfine-shifted exchangeable protons and the T_1's for two heme methyl signals were determined for sperm whale metmyoglobin cyanide in H_2O solution. In the absence of saturation transfer from the suppressed H_2O signal, the determined recovery times for the exchangeable protons represent intrinsic T_1's. The ratios of exchangeable proton T_1's to methyl T_1's yield relative r^{-6} values, which, with the known distance for the heme methyl, result in assignment of the exchangeable imidazole proton for the proximal and distal histidines, the proximal histidine peptide NH, and, most likely, the imidazole NH of His FG2. At 40 °C, pH-dependent saturation transfer factors determined by Redfield experiments and line width analysis permitted the characterization of the exchange rates and mechanisms for the four assigned exchangeable protons. The dominant base-catalyzed proximal histidyl imidazole NH is consistent with the coordination of the imidazole to the iron. A dominant acid-catalyzed proton-exchange mechanism for the distal suggests a hydrogen bond to the coordinated cyanide ligand, which is also supported by the short distance of the exchangeable proton from the iron.

The investigation of numerous structure–function relationships in hemoproteins utilizing proton nuclear magnetic resonance is considerably simplified in the paramagnetic forms of these molecules. In this form, the short-ranged electron–nuclear interactions yield sizable hyperfine shifts which permit resolution of the peaks for the nuclei at the active site.[2] Detailed interpretation of the hyperfine shifts and their dependence on physiological factors, however, depends critically on the unambiguous assignment of the resolved resonances. While this is readily

(1) On leave from the Department of Physics, Southern Illinois University, Carbondale, IL.

(2) Morrow, J. S.; Gurd, F. R. N. *CRC Crit. Rev. Biochem.* **1975**, *3*, 221–287; La Mar, G. N. In "Biological Applications of Magnetic Resonance"; Shulman, R. G., Ed.; Academic Press: New York, 1979; pp 305–343.

0002-7863/81/1503-3567$01.25/0 © 1981 American Chemical Society

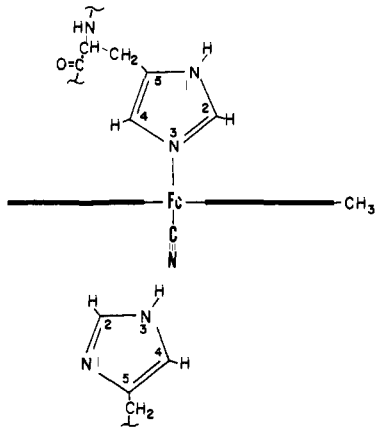

Figure 1. Geometry for the proximal and distal histidyl imidazoles in the heme pocket of sperm whale metmyoglobin cyanide.

achieved for the heme protons of *b*-type hemoproteins via reconstitution of specifically isotope-labeled hemes,[2-8] definitive assignments for resonances arising from protein residues, particularly those coordinated to the heme iron,[2,9-13] are much more elusive.

The importance of the location and assignment of resonances from the ubiquitous proximal and distal histidines is underscored by their proposed focal role in modulating the reactivity of the iron center.[14-16] Since the electron-nuclear interactions are short ranged, the exchangeable resonances of the proximal and distal histidines, particularly those of the imidazole N_1H or N_3H, are probably the most readily assignable. Figure 1 shows these imidazole protons for metmyoglobin cyanide. Single, uniquely hyperfine-shifted resonances directly attributable to the proximal histidyl imidazole N_1H are observed in both deoxy- and aquometmyoglobin.[9,11,12] However, the sizable magnetic anisotropy and concomitant dipolar shifts lead to numerous hyperfine-shifted peaks due to exchangeable protons in cyanometmyoglobin,[9] an excellent model for the ligated state of myoglobin. The early work of Sheard et al.[9] led to a tentative assignment of four of the strongly shifted peaks largely on the basis of a semiquantitative assessment of the expected dipolar and contact contribution to the shifts and a comparison of myoglobins from several species. In view of the inadequate current understanding of the magnitude of the axial and rhombic anisotropies in low-spin ferric systems, an alternative or additional method for assignment is desirable.

Such an approach is provided in the analysis of dipolar relaxation[17] induced in nuclei in the heme cavity. Since diamagnetic proton-proton dipolar relaxation dominates the line width even in low-spin ferric systems, analysis of line widths has serious shortcomings. However, spin-lattice relaxation solely due to diamagnetic effects is relatively ineffective, particularly at high fields,[18] so that measurements of paramagnetic-dominated spin-lattice relaxation times, T_1's, could yield the desired structural information.[17] In such a paramagnetic system, the dominant contribution to T_1^{-1} is given by[17]

$$T_{1i}^{-1} = Dr_i^{-6}f(\tau) + C(A/\hbar)^2 f'(\tau') \quad (1)$$

where the terms D and C represent dipolar and scalar relaxation by the iron unpaired spins, respectively. In the favorable case where $A/\hbar \sim 0$ or at least is small compared to the first term in eq 1, the ratio of T_1's for two nonequivalent protons is given by

$$T_{1i}/T_{1j} = r_i^6/r_j^6 \quad (2)$$

Determination of the T_1 ratio for two peaks for which r_j is known leads directly to r_i.

The determination of T_1's for exchangeable proton resonances, which must be carried out in H_2O rather than ^2H_2O solution, however, requires the saturation of the dominant H_2O signal. If the lifetime of the exchangeable proton in the protein environment, τ_i, is comparable to its T_1, then the intensity of the protein proton signal is influenced by transfer of saturation from the solvent. The loss of intensity through saturation transfer affords a direct method of monitoring the dynamic properties of exchangeable resonances.[19] In view of the significant current interest in the dynamic behavior of proteins in general and the possibility that the nature of fluctuations in structure in myoglobin and hemoglobin[20-22] determine the ease of access and exit of dioxygen to the structurally blocked heme cavity portrayed in crystal structure,[23,24] an exploration of the kinetic lability of exchangeable protons could prove useful. Moreover, the diverse kinetics and mechanism of exchange for different exchangeable protons may provide additional support for the assignments reached on the basis of T_1 measurements.

The exchange rate is derived[19] from solvent saturation transfer from the intrinsic T_1 and the saturation factor, F, given by

$$F = I/I_\circ = T_1^{-1}/(T_1^{-1} + \tau_i^{-1}) \quad (3)$$

where I and $I_\circ$ are the intensities of an exchangeable proton resonance with and without saturating the H_2O signal, respectively. The independent determination[19] of F and T_1 leads directly to τ_1^{-1}. Slightly faster rates can also be monitored by the more conventional analysis of the exchange contribution to line width[25] in the slow exchange limit, according to

$$\pi\delta_i = \pi\delta_{\circ i} + \tau_i^{-1} \quad (4)$$

where δ_i and $\delta_{\circ i}$ are the observed line width and the line width in the absence of exchange, respectively.

We report here on a detailed study of the relaxation properties of the four strongly shifted exchangeable proton resonances as

(3) Mayer, A.; Ogawa, S.; Shulman, R. G.; Yamane, T.; Cavaleiro, J. A. S.; Rocha Gonsalves, A. M. d'A.; Kenner, G. W.; Smith, K. M. *J. Mol. Biol.* **1974**, *86*, 749-756.
(4) La Mar, G. N.; Budd, D. L.; Viscio, D. B.; Smith, K. M.; Langry, K. C. *Proc. Natl. Acad. Sci. U.S.A.* **1978**, *75*, 5755-5759.
(5) La Mar, G. N.; Smith, K. M.; Gersonde, K.; Sick, H. *J. Biol. Chem.* **1980**, *255*, 66-70.
(6) La Mar, G. N.; de Ropp, J. S.; Smith, K. M.; Langry, K. C. *J. Am. Chem. Soc.* **1980**, *102*, 4833-4835.
(7) La Mar, G. N.; de Ropp, J. S.; Smith, K. M.; Langry, K. C. *J. Biol. Chem.* **1980**, *255*, 6646-6652.
(8) La Mar, G. N.; Smith, K. M.; de Ropp, J. S.; Burns, P. D.; Langry, K. C.; Gersonde, K.; Sick, H.; Strittmater, P., In "Proceedings of the Symposium on Interaction Between Iron and Proteins in Oxygen and Electron Transport"; Ho, C., Ed.; Elsevier: Holland, 1980, in press.
(9) Sheard, B.; Yamane, T.; Shulman, R. G. *J. Mol. Biol.* **1970**, *53*, 35-48.
(10) Ogawa, S.; Shulman, R. G.; Yamane, T. *J. Mol. Biol.* **1972**, *70*, 291-300.
(11) La Mar, G. N.; Budd, D. B.; Goff, H. *Biochem. Biophys. Res. Commun.* **1977**, *77*, 104-110.
(12) La Mar, G. N.; Budd, D. B.; Sick, H.; Gersonde, K. *Biochim. Biophys. Acta* **1978**, *537*, 270-283.
(13) La Mar, G. N.; de Ropp, J. S. *Biochem. Biophys. Res. Commun.* **1979**, *90*, 36-41.
(14) Perutz, M. F.; Ten Eyck, L. F. *Cold Spring Harbor Symp. Quant. Biol.* **1971**, *36*, 295-310.
(15) Chevion, M.; Salhany, J. M.; Castillo, C. L.; Peisach, J.; Blumberg, W. E. *Isr. J. Chem.* **1977**, *15*, 311-316.
(16) Valentine, J. S.; Sheriden, R. P.; Allen, L. C.; Kahn, P. *Proc. Natl. Acad. Sci. U.S.A.* **1979**, *76*, 1009-1013.
(17) Swift, T. J. In "NMR of Paramagnetic Molecules"; La Mar, G. N.; Horrocks, Jr., W. D.; Holm, R. H., Eds.; Academic Press: New York, 1973, pp 53-83.
(18) Wüthrich, K. "NMR in Biological Research; Peptides and Proteins"; North-Holland/American Elsevier: Amsterdam, 1976; Chapter IV.
(19) Krishna, N. R.; Huang, D. H.; Glickson, J. D.; Rowan III, R.; Walter, R. *Biophys. J.* **1979**, *26*, 345-366.
(20) Case, D. A.; Karplus, M. *J. Mol. Biol.* **1979**, *132*, 343-368.
(21) Frauenfelder, H; Petsko, G. A.; Tsernoglou, D. *Nature (London)* **1979**, *280*, 558-563.
(22) Englander, S. W.; Calhoun, D. B.; Englander, J. J.; Kallenbach, R. K.; Liem, H.; Malin, E.; Mandal, C.; Rogero, J. R. *Biophys. J.* **1980**, *32*, 577.
(23) Perutz, M. F.; Matthews, F. S. *J. Mol. Biol.* **1966**, *21*, 199-202.
(24) Takano, T. *J. Mol. Biol.* **1977**, *110*, 537-568.
(25) Carrington, A.; McLachlan, A. D. "Introduction to Magnetic Resonance"; Harper and Row: New York, 1967; Chapter 12.

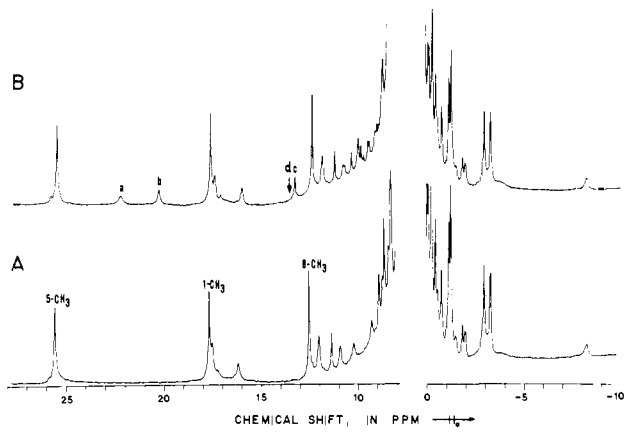

Figure 2. 360-MHz ^1H NMR spectrum of the resolved resonances of sperm whale metMbCN at 40 °C, pH 8.56 in 0.2 M NaCl. (A) ^2H_2O and (B) 90% H_2O/10% ^2H_2O with the H_2O signal saturated. The previous methyl assignments are included in A. Three of the four exchangeable proton signals of interest are labeled a–c in B; the position of d is indicated by an arrow. The intense, largely unresolved diamagnetic region is omitted.

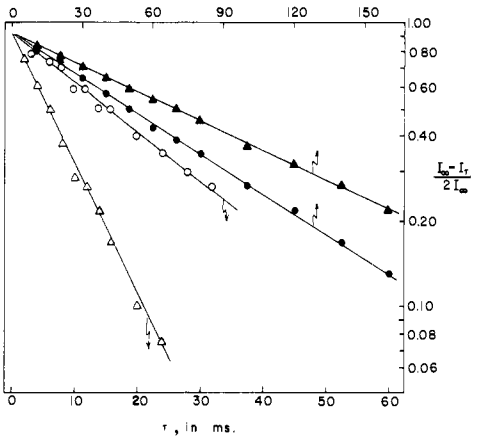

Figure 3. Plots ln $(I_\infty - I_\tau)/2I_\infty$ vs. τ for a 180°–τ–90° sequence T_1 determination for 1-CH_3 (▲), 5-CH (●), peak a (△), and peak b (○) of metMbCN in 90% H_2O at 25 °C, pH 8.56. The saturation factor for peaks a and b is essentially unity under these conditions. The data for 1-CH_3, 5-CH_3, and peaks a and b refer to the upper and lower scales in τ, respectively.

well as selected assigned heme resonances in metmyoglobin cyanide. This study permits both quantitative confirmation of the assignment of the proximal and distal histidyl imidazole exchangeable protons and provides the kinetics and mechanism of exchange with solvent for the labile protons, information which can be interpreted in terms of the dynamic stability of the heme pocket.

Experimental Section

Sperm whale myoglobin was purchased from Sigma as a salt-free, lyophilized powder. The protein was used without further purification.[26] Solutions were prepared in either 99.8% ^2H_2O or 90% H_2O/10% ^2H_2O (for the lock) by dissolving 26 mg of myoglobin in 0.4 mL of solvent, which was 0.2 M in NaCl. The solution was centrifuged to remove any precipitate, a ninefold excess of KCN was added, and the pH was adjusted by the addition of 0.2 M HCl or NaOH (90% H_2O/10% ^2H_2O). The pH was measured directly within the 5-mm NMR tubes by using the Ingold microcombination electrode in conjunction with a Beckman Model 3550 pH meter. The pH readings in ^2H_2O solution are uncorrected for the isotope effect.

All proton NMR spectra were recorded at 360 MHz on a Nicolet NT-360 quadrature FT NMR spectrometer. The complete spectra of metmyoglobin cyanide, metMbCN, in H_2O and ^2H_2O were recorded by using a 10-μs 90° pulse over a 12-kHz bandwidth with 8K data points. The strong solvent resonance in H_2O solution was suppressed by a 30-ms phase-alternated presaturation pulse. The pH of the solution was selected so that the exchangeable proton resonances exhibited minimum saturation transfer (pH ~8.56).

The T_1's for two of the heme methyls and three of the furthest downfield exchangeable proton resonances were determined in H_2O solution by the conventional 180°–τ–90° pulse sequence,[27] with the H_2O resonance saturated at all times except during acquisition. Care was taken to obtain intrinsic T_1's for the exchangeable proton peaks under conditions of no saturation transfer (i.e., $F = 1.0$ in eq 3, so that $\tau_i^{-1} \ll T_1^{-1}$). The T_1 was computed by a nonlinear least-squares fit to the equation $(I_\infty - I_\tau)/2I_\infty = A\exp(-\tau/T_1)$, where I_τ and I_∞ are the intensities of the resonance τ and $>5T_1$ after the 180° pulse and τ is the delay, in milliseconds, between the 180° and 90° pulses. The uncertainties quoted for T_1's correspond to two or more standard deviations as provided from the computer fit. The measurements were found reproducible to better than 7%. In cases when $F \neq 1.0$ in eq 3, the apparent relaxation rate[19] is $T_1^{-1} + \tau_1^{-1}$ if the H_2O peak is kept saturated. Line widths of resonances were measured as full-width at half-length and are given in hertz; all line widths contain a constant 3 Hz introduced by apodization in order to improve the signal/noise ratio.

The degree of solvent saturation transfer to individual exchangeable proton resonances in the protein was determined by comparing the intensities of a resonance in a pair of identically collected Redfield 2-1-4 spectra.[28] In one trace the nonexcited H_2O resonance was saturated by the proton decoupler; in the companion reference spectrum the decoupler frequency was offset downfield from the resonance of interest to where there are no protein peaks. In the reference spectrum the downfield offset was chosen so that the decoupler and the H_2O resonance were symmetrically positioned with respect to peak b (see Figure 2). This choice helps to reduce the effects of decoupler power directly saturating the peaks of interest. The resulting pair of spectra produced identical intensities for all nonexchangeable resonances. For example, the optimal detection of the furthest downfield exchangeable peaks by the Redfield method required 2000 scans using a 20-μs pulse. Intensities were found to be reproducible to within 5–7%, indicating that intensity ratios are certain to better than ±15%. Peak positions are given in parts per million from internal 2,2-dimethyl-2-silapentane-5-sulfonate (DSS) with downfield shifts taken as positive.

Table I. Intrinsic Spin–Lattice Relaxation Times for Selected Protons in metMbCN in 90% H_2O/10% ^2H_2O[a]

	25 °C	40 °C	
resonance	pH 8.56	pH 7.95	pH 9.19
a	9.31 ± 0.26	*c*	9.88 ± 0.14
b	25.5 ± 1.5	24.8 ± 0.5	*d*
c	*b*	114 ± 2	*e*
1-CH_3	115 ± 2	126 ± 2	123 ± 2
5-CH_3	81.6 ± 1.0	86.3 ± 0.8	87.9 ± 0.6

[a] T_1's in milliseconds. The ± values denote ⩾ two standard deviations (see Experimental Section). [b] Not determined due to overlap with peak d. [c] Effective T_1 = 4.7 ± 0.2 ms, including a contribution from exchange. [d] Effective T_1 = 17.8 ± 0.3 ms, including a contribution from exchange. [e] Effective T_1 = 93.7 ± 1.5 ms, including a contribution from exchange.

Results

The 360-MHz proton NMR spectra of sperm whale metMbCN in ^2H_2O and 90% H_2O/10% ^2H_2O are illustrated in A and B of Figure 2, respectively; the previously determined heme methyl assignments[3] are included in Figure 2A. Optimal resolution of the desired peaks is achieved at 40 °C. The spectra are essentially the same as those reported earlier[9] at 220 MHz except for significantly improved resolution in the crowded region 9–12 ppm, where there appear at least seven exchangeable peaks in addition to the four marked a–d, which had been considered previously. Peak d is not observable in Figure 2 because the H_2O resonance

(26) Sperm whale myoglobin contains three components, as identified by disc electrophoresis (Antonini, E.; Brunori, M., "Hemoglobin and Myoglobin in Their Reactions with Ligands"; North-Holland: Amsterdam, 1971; pp 6–9), with essentially identical ligand-binding properties; the major component comprises 85–90%, with two lesser components of ~10–15% and <5%. The minor component can be resolved by NMR at certain pH values, indicating the major component is present at ⩾90%.

(27) Farrar, T. C.; Becker, E. D., "Pulse and Fourier Transform NMR"; Academic Press: New York, 1971.

(28) Redfield, A. G.: Kunz, S. D.; Ralph, E. K. *J. Magn. Reson.* **1975**, *19*, 116–117.

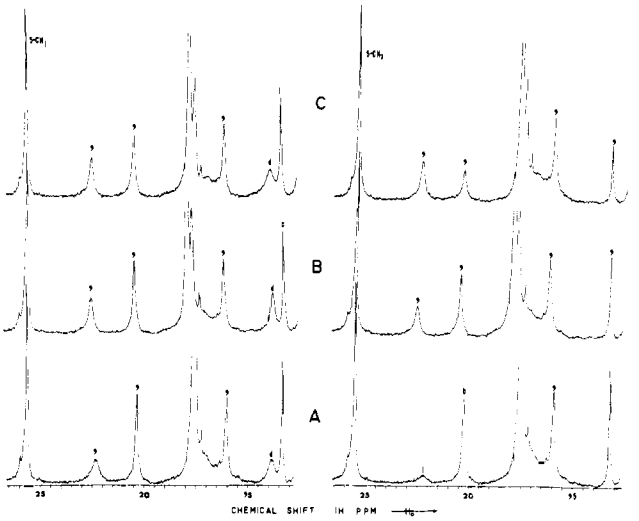

Figure 4. 360-MHz Redfield 2-1-4 ^1H NMR traces for the region 13–26 ppm downfield from DSS for sperm whale metMbCN at 40 °C in 0.2 M NaCl. (A) pH 7.95, (B) pH 8.58, (C) pH 9.53. The traces on the left have the decoupler offset downfield ~5 kHz from the peaks of interest and the water nonexcited; the traces on the right correspond to the spectra on the left except that the decoupler is set on the H_2O resonance so as to completely saturate it. Peak d, which is always suppressed when water is saturated (i.e., B in Figure 2), can be clearly seen on the left. x designates a nonexchangeable single proton heme resonance, probably a propionic acid H_α.

is being saturated, but can be seen via the Redfield method (vide infra). Its position is indicated by a vertical arrow. Under the condition of presaturating the H_2O peak in Figure 2B, several of the seven exchangeable resonances in the region 9–11 ppm are also suppressed by saturation transfer. However, since the exchangeable resonances in this region are not yet assignable and determination of their relaxation times and quantitative saturation factors is severely hampered by the erratic base line so close to the irradiated H_2O signal, we will focus here solely on the well-resolved exchangeable proton resonances downfield from 8-CH_3.

The plot of ln $[(I_\infty - I_\tau)/2I_\infty]$ vs. τ for 1-CH_3, 5-CH_3, and peaks a and b at 25 °C and pH 8.56 is presented in Figure 3, and the resulting T_1's are listed in Table I. Peaks *a* and *b* exhibit essentially their full intensities at this pH and temperature so that the slopes indicate intrinsic T_1 values free of exchange effects. T_1 determinations were similarly made at 40 °C at pH 7.95 and 9.19, and the values are also included in Table I. At the lower pH, true T_1 values are obtained only for the methyls and peaks b and c, while at the higher pH only peak a yields a true T_1 value (vide infra). The T_1's for each methyl increase with higher temperature, as expected, and the values are unaffected by pH in the measured range.

In A, B, and C of Figure 4 we present the pairs of Redfield 2-1-4 spectra[28] of the downfield region at pH values of 7.95, 8.58, and 9.53, respectively. In each case the trace on the left corresponds to the normal situation with a nonexcited H_2O peak. The traces on the right represent the same spectra but with the H_2O signal completely saturated. The known nonexchangeable resonances (i.e., 5-CH_3 and the single proton peak at 16 ppm (marked x), as well as the truncated 1-CH_3 and 8-CH_3) have identical intensities. Peak d is completely suppressed via saturation transfer at all pH values. At the lowest pH only peak a exhibits reduced intensity, while at the highest pH only peak a retains its complete intensity. The saturation factor for peaks a–c, as defined in eq 3, are plotted as a function of pH at 40 °C in Figure 5. A portion of the data on peak b has been discussed elsewhere.[29] Clearly peak a experiences saturation transfer only at acidic pH, while peaks b and c exhibit saturation transfer only at alkaline pH; F = 0 at all pH values for peak d.

(29) La Mar, G. N.; Cutnell, J. D.; Kong, S. B. *Biophys. J.* **1981**, *34*, 217–226.

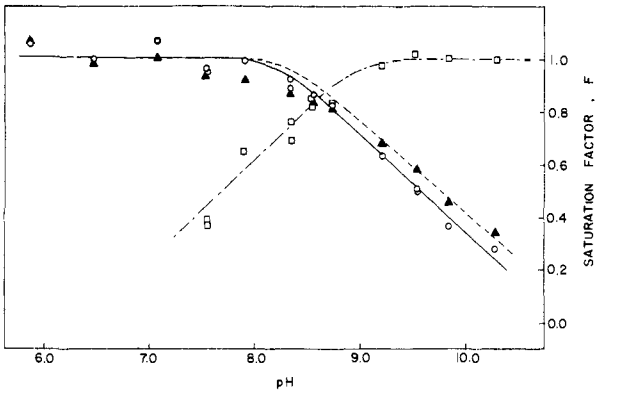

Figure 5. Plots of the saturation factor, $F = I/I_\circ$, for the exchangeable peaks a (□), b (○) and c (▲) of metMbCN in 0.2 M NaCl at 40 °C, as a function of pH. The lines have no theoretical significance and are simply to indicate trends.

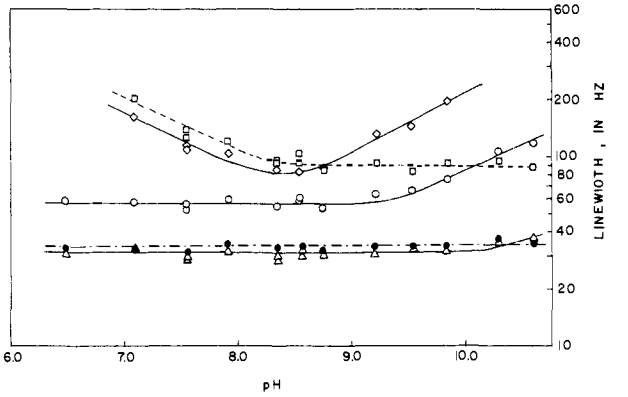

Figure 6. Semilog plot of line width, δ, as a function of pH for 5-CH_3 (●), a (□), b (○), c (△), and d (◇) for sperm whale metMbCN in 0.2 M NaCl in 90% H_2O/10% ^2H_2O at 40 °C.

The line widths at 40 °C as a function of pH for the four exchangeable proton peaks a–d and best resolved methyl, 5-CH_3, are illustrated in Figure 6. The nonexchangeable 5-CH_3 (as well as 1-CH_3 and 8-CH_3) exhibits a completely pH-independent line width, δ (T_2's, with $T_2 = (\pi\delta)^{-1}$), over the range 6.5–10.6, which is consistent with a unique conformation and invariant electronic structure of the heme.[9,12] Peak a has a pH-independent line width in the range 8.5–10.5; below pH 8.5 the line width increases. Peak b has a constant δ to pH 9, after which it increases with increase in pH. Peak c shows an effect similar to that of peak b, although to a much lesser degree. On the other hand, peak d has a minimum linewidth at pH ~8.4, with δ increasing with either increasing or decreasing pH.

In view of the pH-independent shifts and constant line widths for nonexchangeable peaks, the pH-dependent line width contributions for the exchangeable peaks must represent the onset of exchange effects[25] in the NMR slow-exchange region, where the exchange rate can be readily determined by eq 4; the nonexchanging line width contribution is given by the pH-independent portion of the line width vs. pH value plot. In peak d no pH-independent line width region is observed, making estimates to $\delta_\circ$ more indirect. Upon lowering the temperature at pH 8.56, where exchange effects are minimized for peak d, the peak narrows dramatically, approaching a limiting line width approximately 20% larger than that for peak c. Hence, we estimate $\delta_\circ$ for d as 38 Hz.

The exchange rates from saturation factors are determined by using eq 3 and assuming that the intrinsic T_1's are independent of pH as given in Table I at 40 °C. The assumption of pH-independent T_1's appears well founded in view of the identical T_1's for methyls at two different pH values and the pH-invariant T_1's where there are no exchange contributions (i.e., δ's in Figure 6). The resulting rates, τ_1^{-1}, are plotted as a function of pH in Figure

Table II. Assignment of Exchangeable Proton Resonance Based on Relative Relaxation Times

peak designation	peak assignment	X-ray structural data[a] $r(H_i)$, Å	X-ray structural data[a] $r(H_i)/r(CH_3)$	observed[b] $[T_1(H_i)/T_1(1\text{-}CH_3)]^{1/6}$
a	His E7 N_3H (distal)	4.2	0.67	(0.66–0.70) ± 0.02
b	His F8 N_1H (proximal)	5.1	0.81	(0.77–0.82) ± 0.03
c	His F8 peptide NH	6.9	1.10	(0.98–1.04) ± 0.03
d	His FG2 N_3H	5.6	0.89	*c*
$1\text{-}CH_3$		6.2	1.00	
	Ser F7 OH	5.8	0.92	*d*

[a] References 9, 33. [b] Sixth root (eq 1) of T_1 ratios in Table I; uncertainties represent only uncertainties in T_1's; the range is determined by possible magnetic anisotropy;[32] the lower value arises solely from $^6\sqrt{T_i/T_j}$ and the upper value arises from $^6\sqrt{(g_{\parallel}^2 + g^2)/(g^2 + g^2)T_i/T_j}$, so that depending on the actual anisotropy, all values in between can occur (ref 32). [c] T_1 could not be determined since $F = 0.0$ for all pH values. [d] Peak predicted[3] to experience too small a hyperfine shift to resonate downfield of 10 ppm.

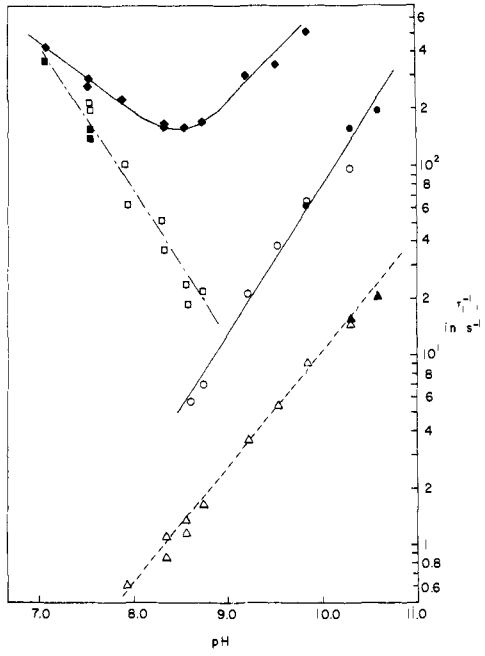

Figure 7. Plot of the log of the exchange rate, τ_i^{-1}, for peaks a (□–■), b (○–●), c (△–▲), and d (♦) as a function of pH at 40 °C for metMbCN in 0.2 M NaCl in 90% H_2O/10% ^2H_2O. The open markers are derived from the saturation factors (eq 3) and the solid markers are obtained from line width data (eq 4). The straight lines for peaks a–c are least-squares fits to all the data points for a given peak.

7. The open markers represent the data from saturation factors, while the solid markers derive from the analysis of the pH-dependent line widths. A single straight line can be drawn through both the line width and saturation factor derived data points for a given resonance, as illustrated in Figure 7.

Discussion

Assignment of Resonances. The relaxation data for the two heme methyls in Table I reveal that $5\text{-}CH_3$ is relaxed slightly more efficiently than $1\text{-}CH_3$. Since $\langle r^6 \rangle$ in eq 2 for the four methyls must be the same, and the most efficient relaxation occurs for the peak with the largest shift, we conclude that scalar relaxation (second term in eq 1) also makes some contribution to the overall T_1 of at least $5\text{-}CH_3$. A similar effect has been demonstrated[30] in model complexes for metMbCN, where heme methyl peaks with hyperfine shifts of >15 ppm exhibited relaxation rates which increased with shift. For hyperfine shifts <15 ppm, dipolar relaxation dominated overwhelmingly.[30] Thus we assume that T_1 for $1\text{-}CH_3$ is essentially dipolar. Since the hyperfine shifts for peaks a–d are comparable or smaller[31] than for $1\text{-}CH_3$, we assume that only the first term in eq 1 is important. Under these circumstances eq 2 is valid,[32] and by using the estimated $\bar{r} = (\langle r^6 \rangle)^{1/6} = 6.2$ Å derived from X-ray data of protoporphyrin complexes, we can obtain the ratio $r(H_i)/\bar{r}(CH_3)$ from X-ray data[33] and from comparison with the experimental $[T_1(H_i)/T_1(1\text{-}CH_3)]^{1/6}$, as listed in Table II.

As seen in Table II, the relaxation behavior of peak b is consistent only with the N_1H of the proximal histidine as its origin. Similarly, the much faster relaxation of peak a and the resulting short distance of ~4.2 Å dictate that it comes from the distal residue, the N_3H of His E7. The assignments for peaks a and b are unique and unambiguous and agree completely with the earlier proposal by Sheard et al.[9] on the basis of estimated dipolar shifts. The distal histidine assignment is independently confirmed by the observation[34] that peak a is missing in metMbCN from elephant, which has the distal histidine E7 replaced with a glutamine;[35] peak b is still present with essentially unaltered relaxation and exchange properties.[34] The relaxation behavior of peak c is not inconsistent with the earlier assignment[9] to the peptide NH of His F8. The inability to obtain T_1 data for peak d and the probable dominance of diamagnetic effects on line width preclude a unique assignment based on relaxation data. However, the presence[9] of a small but definite temperature coefficient to the shift leads us to its assignment to N_3H of His FG2, which lies parallel and in contact to the heme on the proximal side. The small shift for a proton so close to the iron is due to the location of the proton at the magic angle, as discussed before.[9] This assignment is supported by qualitative relaxation data in that it is observed that the line width of peak d is always greater than that for peak *c*, indicating that proton d is closer than 6.9 Å.

While the assignment for peak d is not unambiguous, due to the absence of T_1 data, our analysis demonstrates that determination of T_1 values for exchangeable resonances in hemoproteins can provide a quantitative basis for assigning the resonances for at least the residues closest to the iron, i.e., the proximal and distal residues. We have succeeded in assigning by these means the proximal histidyl imidazole N_1H peak in a wide variety of low-spin ferric hemoproteins,[36] and we believe the method should have

(30) La Mar, G. N.; Viscio, D. B.; Smith, K. M.; Caughey, W. S.; Smith, M. L. *J. Am. Chem. Soc.* **1978**, *100*, 8085–8092.

(31) Although peaks a and b are downfield from $1\text{-}CH_3$, they have smaller hyperfine shifts because the diamagnetic position for $1\text{-}CH_3$ is ~3.6 ppm, while the NH for imidazole resonates ~10 ppm from DSS (ref 9).

(32) Actually, in a magnetically anisotropic system which possesses primarily axial anisotropy, as is likely the case in metMbCN, the pertinent eq 2 should be $T_i/T_j = [\bar{g}^2 + g_{\parallel}^2 \cos^2\theta_j + g_{\perp}^2 \sin^2\theta_j]r_i^6/[\bar{g}^2 + g_{\parallel}^2 \cos^2\theta_i + g_{\perp}^2 \sin^2\theta_i]r_j^6$ (Sternlicht, H. J. *Chem. Phys.* **1965**, *42*, 2250–2251), where θ is the angle between the Fe–H_i vector and the heme pseudo-fourfold axis. In comparison of the heme methyl ($\theta = 90$) with either the proximal or distal histidyl imidazole NH's which are nearly on the unique axis ($\theta \sim 0$), eq 2 becomes $T_{1i}/T_{1j} = [r_i^6/r_j^6](\bar{g}^2 + g_{\parallel}^2)/\bar{g}^2 + g_{\perp}^2)$, and the distance ratio in Table II becomes $r(H_i)/r(CH_3) = [(\bar{g}^2 + g_{\perp}^2)/(\bar{g}^2 + g_{\parallel}^2)] \times T_1(H_i)/T_1(CH_3)]^{1/6}$. Since for low-spin ferric hemes $g_{11} > g_{\perp}$, $r(H_i)/r(CH_3)$ determined solely on the basis of T_1's is necessarily smaller than the true ratio. If we assume an axial anisotropy which gives, at maximum, a ~6-ppm upfield methyl dipolar shift which is consistent with imidazole/cyanide ligated ferric models (La Mar, G. N.; Del Gaudio, J.; Frye, J. S. *Biochim. Biophys. Acta* **1977**, *498*, 422–435), the individual *g* values can be estimated (Goff, H.; La Mar, G. N.; Reed, C. A. *J. Am. Chem. Soc.* **1977**, *99*, 3641–3646), yielding $[(\bar{g}^2 + g_{\parallel}^2)/(\bar{g}^2 + g_{\perp}^2)] = 1.42$. Thus the r_i values can be small by *up to* 6% on the basis of eq 2.

(33) Kendrew, J. C.; Watson, H. C.; Strandberg, B. E.; Dickerson, R. E.; Phillips, D. C.; Shore, V. C. *Nature (London)* **1961**, *190*, 666–670, and data based on this structure cited in ref 9.

(34) La Mar, G. N.; Kong, S. B., unpublished observations.

(35) Mizukami, H.; Bartnicki, J., to be published.

general applicability to other oxidation/spin states of hemoproteins.

Dynamics of Labile Proton Exchange. The exchange data reflect facile exchange of labile protons of residues buried in the highly hydrophobic interior of the protein. Such exchange is taken as direct evidence that these proteins are not static but undergo fluctuation which exposes these residues to solvent.[22,37] We have already shown elsewhere[29] that the differential exchange rates of the unique proximal histidyl imidazole N_1H in deoxy myoglobin and metmyoglobin cyanide provide evidence for widely differing dynamic stabilization of the heme pocket in ligated and unligated myoglobin. Even more dramatic differences in exchange rates for peptide NH's between unligated and ligated hemoglobin have been reported based on tritium-labeling studies,[22] but the location of the ligation state sensitive proton has yet to be established. Such differential amplitudes of fluctuation could serve as an allosteric control mechanism for O_2 access to and exit from the sterically blocked heme pocket in hemoglobin.

The exchange rate may be generally written[37]

$$\tau_i^{-1} = k_A[H^+] + k_B[OH^-] + k_W[H_2O] \qquad (5)$$

where k_A, k_B, and k_W are the rate constants for acid-, base-, and water-catalyzed exchange of N-H protons. The kinetic data in Figure 7 reveal that peak b exhibits only base-catalyzed exchange, i.e., $k_B \gg k_A$. Since a coordinated imidazole is not susceptible to acid attack unless the Fe-N bond is broken, the dominance of base-catalyzed exchange for the His F8 N_1H should be expected and may be diagnostic for this resonance.

On the other hand, peak a, which is due to the distal His E7 N_3H, exhibits only acid-catalyzed exchange, i.e., $k_A \gg k_B$. Bretscher had already suggested[38] that the N_3H of His E7 is hydrogen bonded to the coordinated cyanide. The determined $r = 4.2$ Å places the proton essentially within the van der Waals contact of the coordinated cyanide, strongly supporting such an interaction. This interaction, depicted in Figure 1, also would stabilize the proton against attack by base, which is consistent with the observed dominance of acid-catalyzed exchange. In the absence of such a strong interaction, exchange of the imidazole NH would be expected to occur by both acid and base catalysis. Such is precisely the case for peak d, assigned to His FG2. Peak c exhibits a much slower exchange rate than peaks a or b, consistent with the reduced lability of peptide protons,[37] which also generally feature $k_B \gg k_A$.

The slopes to the straight ines fit by a least-squares method to the data points for each resonance in Figure 7 yield slopes of 0.79 ± 0.08 for peak a, 0.77 ± 0.09 for peak b, and 0.63 ± 0.07 for peak c. There are insufficient data points to establish the slopes of either the low pH or pH sides for peak d. Thus the exchange rate is less than first order in [OH] (peak b and c) or $[H^+]$ (peak a), an observation which is often taken as evidence[37] for the EX_2 mechanism where the rate of interconversion between a buried (folded) and exposed (more random) orientation for the residue containing the exchanging proton is much faster than the rate of proton exchange with water in the exposed orientation.

Thus, our study of the dynamics of labile proton exchange demonstrates that rates can be determined over a two-decade range and that the exchange behavior with respect to pH provides not only support for some assignments for resonances determined primarily from relaxation time measurements, but also supports the presence of a strong interaction of the distal histidine with the coordinated cyanide. These exchange properties may provide additional definitive structural and/or dynamic information on myoglobin as similar data on related hemoprotein becomes available for comparison. Preliminary studies in these laboratories indicate that the exchange rates by base catalysis of the uniquely assignable proximal histidyl imidazole N_1H varies by over seven decades among such diverse hemoproteins as cytochromes *c* and *c'*, legume hemoglobin, and horseradish peroxidase.[36]

Acknowledgment. This research was supported by a grant from the National Science Foundation (CHE-77-26517), the UCD NMR Facility, and (in part) the National Institutes of Health (HL-16087).

(36) La Mar, G. N.; de Ropp, J. S.; Kong, S. B.; Cutnell, J. D.; Jackson, J. T., to be published.
(37) Woodward, C. K.; Hilton, B. D. *Annu. Rev. Biophys. Bioeng.* **1979**, *8*, 88-127.
(38) Bretscher, P. A. Ph.D. Thesis, Cambridge University, England, 1968.

Communications to the Editor

Versatility of Mo(*t*-BuS)$_4$. Selective Formation of a Series of Thiolatomolybdenum(I), -molybdenum(II), and -molybdenum(IV) Compounds

Masato Kamata, Toshikatsu Yoshida, and Sei Otsuka*

Department of Chemistry, Faculty of Engineering Science Osaka University, Toyonaka, Osaka 560, Japan

Ken Hirotsu and Taiichi Higuchi*

Department of Chemistry, Osaka City University Sumiyoshiku, Osaka 558, Japan

Received February 12, 1981

Despite considerable current interest in thiolatomolybdenum compounds due to their possible implication in redox-active molybdoenzymes,[1,2] substitution active molybdenum compounds ligated with unidentate thiolate remain rare. Recently we were able to prepare a novel homoleptic compound, Mo(*t*-BuS)$_4$ (**1**).[3] This compound exhibits remarkable reactivity toward various reagents ranging from nucleophiles to electrophiles. Here we wish to report the reactions with CO, *t*-BuNC, and PMe_2Ph,[4] typical biphilic reagents varying in electronic properties.

To a stirring solution of **1** (3.5 mmol) in *n*-hexane (45 mL) was added *t*-BuNC (16.5 mmol) at ambient temperature. The initial red solution rapidly turned dark green. The solution was allowed to stand for 1 h during which time a dark green crystalline product precipitated. The mixture being cooled below −10 °C, the precipitate was collected by filtration and washed with cold *n*-hexane to remove *t*-BuSS(*t*-Bu) and unreacted *t*-BuNC. The solid product, which was found to be Mo(*t*-BuS)$_2$(*t*-BuNC)$_4$ (**2**) (85% yield), thus obtained is pure enough for further chemical trans-

$$\underset{\mathbf{1}}{\text{Mo}(t\text{-BuS})_4} + 4t\text{-BuNC} \rightarrow \underset{\mathbf{2}}{cis\text{-Mo}(t\text{-BuS})_2(t\text{-BuNC})_4} + t\text{-BuSS}(t\text{-Bu}) \quad (1)$$

(1) Reviews: (a) Stiefel, E. I. *Progr. Inorg. Chem.* **1977**, *22*, 1. (b) Kuehn, C. G.; Isied, S. S. *Ibid.* **1980**, *27*, 153-221.
(2) Newton, W. E., Otsuka, S., Eds. "Molybdenum Chemistry of Biological Significance"; Plenum Press: New York, 1980.
(3) Otsuka, S.; Kamata, M.; Hirostu, K.; Higuchi, T. *J. Am. Chem. Soc.* **1981**, *103*, 3011.
(4) All reactions are described here (except the reaction under a CO pressure) were carried out under a pure nitrogen atmosphere employing dry deaerated solvents.

0002-7863/81/1503-3572$01.25/0 © 1981 American Chemical Society